CARBON 49 (2011) 3709–3716

available at www.sciencedirect.com

ScienceDirect

journal homepage: www.elsevier.com/locate/carbon

Nanotube fracture during the failure of carbon nanotube/alumina composites

Go Yamamoto [a,b,*], Keiichi Shirasu [b], Toshiyuki Hashida [b], Toshiyuki Takagi [a], Ji Won Suk [c], Jinho An [c], Richard D. Piner [c], Rodney S. Ruoff [c]

[a] Institute of Fluid Science, Tohoku University, Sendai 980-8577, Japan
[b] Fracture and Reliability Research Institute, Tohoku University, Sendai 980-8579, Japan
[c] Department of Mechanical Engineering and the Texas Materials Institute, University of Texas, Austin, TX 78712, USA

ARTICLE INFO

Article history:
Received 24 February 2011
Accepted 10 April 2011
Available online 15 April 2011

ABSTRACT

Multi-walled carbon nanotubes (MWCNTs) underwent failure during crack opening in a MWCNT/alumina composite. Transmission electron microscope observations and single nanotube pullout tests revealed that the MWCNTs, rather than pulling out from the alumina matrix, broke in the outer shells and then the inner core was pulled away, leaving fragments of the outer shells in the matrix (i.e., they underwent failure in a "sword-in-sheath" fracture mode, as observed for MWCNTs under tensile loading). Some MWCNTs failed leaving either a very short sword-in-sheath failure or a clean break. Theoretical predictions based on the MWCNT failure and pullout models suggested that the use of MWCNTs having a much higher load carrying capacity may lead to composites with a higher fracture toughness. These results may provide new insight into the fracture mechanisms and suggest a new design methodology for MWCNT-based ceramic composites, leading to improved fracture toughness.

1. Introduction

Advanced engineering ceramics such as Al_2O_3, Si_3N_4, SiC and ZrO_2 produced by conventional manufacturing technology have high stiffness, excellent thermostability and relatively low density, but extreme brittle nature restricted them from many structural applications [1]. In order to overcome the toughness problem, incorporation of particulates, flakes and short/long fibers into ceramics matrix, as a second phase, to produce tougher ceramic materials is an eminent practice for decades [2]. Recently, researchers have focused on the carbon nanomaterials, in particular carbon nanotubes (CNTs), which are nanometer-sized tubes of single- (SWCNTs) or multi-layer graphene (MWCNTs) with outstanding mechanical, chemical and electrical properties [3–7], motivating their use in ceramic composite materials as a fibrous reinforcing agent. Until now, however, most results for strengthening and toughening have been disappointing, and only little or no improvement have been reported in CNT/ceramic composite materials [8,9], presumably owing to the difficulties in homogeneous dispersion of CNTs in the matrix and in formation of adequate interfacial connectivity between two phases.

The strengthening and toughening mechanisms of composites by fibers are now well established [2]; central to an understanding is the concept of interaction between the matrix and reinforcing phase during the fracture of the composite. The fracture properties of such composites are dominated by the fiber bridging force resulting from debonding and sliding resistance, which dictates the major contribution to the strength and toughness. It has been demonstrated through scanning electron microscope (SEM) [10] that the MWCNT/alumina composites exhibits the three hallmarks of

* *Corresponding author at:* Institute of Fluid Science, Tohoku University, Sendai 980-8577, Japan. Fax: +81 22 795 4311.
E-mail address: gyamamoto@rift.mech.tohoku.ac.jp (G. Yamamoto).
0008-6223/$ - see front matter
doi:10.1016/j.carbon.2011.04.022

toughening found in the micron-scale fiber composites; crack deflection at the MWCNT/alumina interface, crack bridging by MWCNT, and MWCNT pullout on the crack plane, which would be effective in improvement of fracture toughness of the brittle ceramics. Therefore, a fundamental understanding of the interfacial nature is essential for making decisions on fundamental materials design of composites with CNTs for higher strength and toughness. Effort has been devoted to understanding the CNT/matrix interface in the fracture process [10–13]. In one study, Wagner and co-workers have investigated the crack bridging behavior of a MWCNT/polymer composite by using a single nanotube pullout technique. A single MWCNT was pulled out from a polyethylene–butene matrix, and MWCNTs were effective as a filler in reinforcing the polymer [13]. Unfortunately, making ceramic composites with CNTs has been a significant challenge [8,9], the understanding of the interfacial nature between CNTs and the ceramics matrix is so far from satisfactory.

This paper explains why previous reports indicated only modest improvements in the fracture properties of MWCNT-based ceramic composites. Here, the failure mechanism of the MWCNTs during crack opening in a MWCNT/alumina composite is investigated through transmission electron microscope (TEM) observations and single nanotube pullout tests. Contradictory to the conventional understanding [10,14], (which have reported that pullout phenomena evidently occurred in the bulk CNT/alumina composites), no pullout behavior was observed, instead MWCNTs broke prior to pullout from the matrix. Achieving tougher ceramic composites with MWCNTs is discussed based on these results.

2. Experimental

The alumina composite made with 0.9 vol.% pristine MWCNTs was prepared by precursor method [15]. Further details of the composite preparation are described elsewhere [16]. The MWCNT material (acquired from Nano Carbon Technologies) was synthesized by a catalytic chemical vapor deposition method followed by high temperature annealing. The diameters and lengths of the pristine MWCNTs from SEM (Hitachi S-4300) and TEM (Hitachi HF-2000) measurements ranged from 33 to 124 nm (average: 70 nm) and 1.1 to 22.5 μm (average: 8.7 μm), respectively. TEM observations revealed that the MWCNTs have a "crystalline" multi-walled structure with a narrow central channel [16,17]. Similar observations have been made by others on this type of MWCNT [18]. The 52 mg pristine MWCNTs were dispersed in 400 ml ethanol with aid of ultrasonic agitation. Aluminum hydroxide 15.2 g (Wako Pure Chemical Industries) was added to this solution and ultrasonically agitated. Seventy-three milligrams of magnesium hydroxide (Wako Pure Chemical Industries) was added to prevent excessive crystal growth of alumina. The resultant suspension was filtered and dried in an air oven at 60 °C. Finally, the product obtained in the previous step was put into a half-quartz tube and was dehydrated at 600 °C for 15 min in argon atmosphere. The composites were prepared by spark plasma sintering (SPS, Sumitomo Coal Mining SPS-1050) in a graphite die with an inner diameter of 30 mm at a temperature of 1500 °C under a pressure of 20 MPa in vacuum for 10 min. In order to compare the physical and mechanical properties of the composites, a MWCNT-free alumina sample was prepared under similar processing conditions.

The single nanotube pullout experiments were carried out using an *in situ* SEM (Quanta 600 FEG; FEI) method with a nanomanipulator system [19]. An AFM cantilever (PPP-ZEILR, nominal force constant 1.6 N/m; NANOSENSORS) was mounted at the end of a piezoelectric bender (ceramic plate bender CMBP01; Noliac) on an *X*–*Y* linear motion stage, and the composite with fracture surface (that was coated with platinum) was mounted on an opposing *Z* linear motion stage. The piezoelectric bender was used to measure the resonant frequency of each cantilever in vacuum. A single MWCNT on the fracture surface was clamped onto a cantilever tip by local electron-beam-induced deposition (EBID) of a carbonaceous material [20]. As a precursor source for the EBID, we used n-docosane ($C_{22}H_{46}$, Alfa Aesar), which was dissolved in toluene to make a 3 mass% solution. A small amount of the solution was dropped on a cut-in-half copper TEM grid. After the solution evaporated, the TEM grid with paraffin source was mounted on the AFM chip, as shown in Fig. 1. The deposition rate of the EBID depends on several factors [20]. Thus, the amount of the paraffin source, deposition time, and distance between the paraffin source and the cantilever tip were experimentally-optimized.

The cantilevers serve as force-sensing elements and the spring constants of each were obtained *in situ* prior to the pullout test using the resonance method developed by Sader et al. [21]. The applied force is calculated from the angle of deflection at the cantilever tip, and the nanotube elongation is determined by counting the numbers of pixels in the acquired SEM images [22]. A crosshead speed – i.e., movement rate of the cantilever – of about 100 nm/s was applied for the pullout tests. The transition from linear to nonlinear deformation of a rectangular cantilever occurs at the deflection of cantilever tip (δ)/cantilever length (L) ratio of around 15% [23]. The largest deflection of 16.6 ± 1.2 μm (the force constant of this cantilever was 1.53 N/m) was observed for the tensile-loading experiment, and the cantilever length (L) employed this experiment was 450.31 ± 0.23 μm. Thus, the δ/L ratio of 3.7 ± 0.3% shows that Sader's method to calibrate the cantilever is reliable.

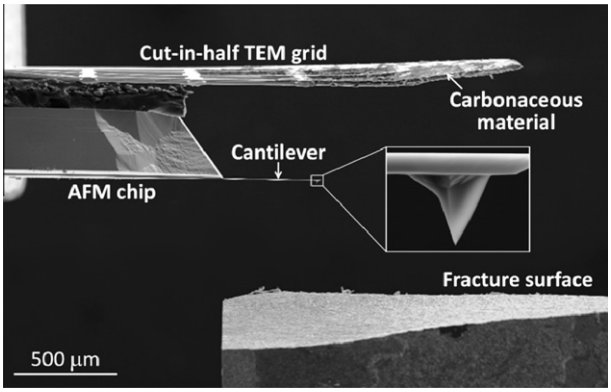

Fig. 1 – SEM image showing the experimental setup for pullout tests.

3. Results and discussion

The physical and mechanical properties, and electrical conductivity of the composite and MWCNT-free alumina sample are shown in Table 1. The details of physical and mechanical evaluations can be found in the Supplementary material. X-ray diffraction analysis of the sintered body revealed that the aluminum hydroxide has been transformed to α-alumina during SPS at 1500 °C under 20 MPa. The aluminum hydroxide powder with 0.9 vol.% pristine MWCNTs can be solidified by SPS to near-theoretical density. Measured bending strength, fracture toughness and Vickers hardness are 543.8 ± 60.9 MPa, 4.74 ± 0.12 MPa $m^{1/2}$ and 17.0 ± 0.4 GPa, respectively.

SEM images shown in Fig. 2 display the morphology of the fracture surface of the composite. From the fracture surface, the following features can be noted. First, as shown in Fig. 2a, the fracture surface of the composite exhibits protruding MWCNTs from the crack flank. Most of MWCNTs are located in the intergranular phase and their lengths are in the range 0–11.8 μm (number average of 160 protruding MWCNTs is 2.8 μm). Second, some MWCNTs are observed to debond from the matrix and leave traces on the fracture surfaces, as exemplified in Fig. 2b. These MWCNTs are partially exposed to the crack plane, and the exposed area of such MWCNTs lie parallel to the crack plane. Therefore, such MWCNTs are less effective at reinforcing, i.e., they are not load bearing during the failure of the composite, and no significant damage may be induced in such MWCNTs during crack opening. Third, the morphology of the fracture surface of the matrix shows clearly the edge and corner fractural feature, indicating that intergranular fracturing took place in the matrix. Its microstructure consisted of equiaxed grains structure with a grain size of 1.43 ± 0.31 μm. In addition to the above features, some MWCNTs on the fracture surface show a clean break near the crack plane, and that the diameter of MWCNT drastically slenderized toward their tip, as illustrated in Fig. 2c and d, respectively. As SEM cannot clearly resolve the thickness of a single MWCNT, TEM was used to determine if the fracture phenomenon of MWCNTs was indeed occurring during crack opening.

TEM observations on the fracture surface demonstrated that a diameter change in the MWCNT structure was evidently observed for a certain percentage of the MWCNTs (Fig. 3a). At least, 25% MWCNT appear to have an apparent diameter change. (The observation was made for 281 MWCNTs.) As shown in Fig. 3b, the high magnification TEM image clearly showed a change in diameter, and this morphology is quite similar to a "sword-in-sheath"-type failure as observed in the failure mode of MWCNTs under tensile loading [7,17,19,24]. Key features are illustrated in enlarged TEM image, taken from the square area in Fig. 3b. The inset showed that outer-walls having approximately 10 shells were observed to break up at location where the MWCNT undergo

Table 1 – The properties of the alumina composite sample with 0.9 vol.% MWCNTs, and of the MWCNT-free alumina sample.

Sample	Composite	Alumina
Relative density (%)	98.9	98.6
Grain size (μm)	1.43 ± 0.31	1.69 ± 0.35
Bending strength (MPa)	543.8 ± 60.9	502.3 ± 19.4
Fracture toughness (MPa $m^{1/2}$)	4.74 ± 0.12	4.37 ± 0.07
Hardness (GPa)	17.0 ± 0.4	17.3 ± 0.5
Young's modulus (GPa)	358.0	357.0
Poisson's ratio	0.20	0.21
Electrical conductivity (S/m)	1.4	10^{-10}–10^{-12}

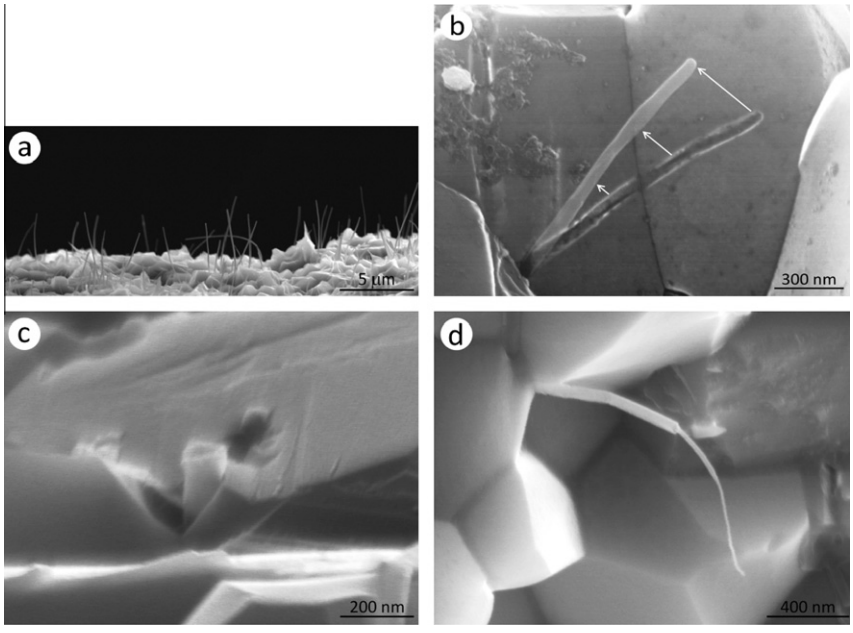

Fig. 2 – SEM images of fracture surface of the composite used for the measurement of bending strength. (a) Numerous individual MWCNTs protrude from the clack plane. (b) Shown is a debonded MWCNT from the matrix that may be not load bearing during crack opening. (c,d) Some MWCNTs have broken in the multi-wall failure.

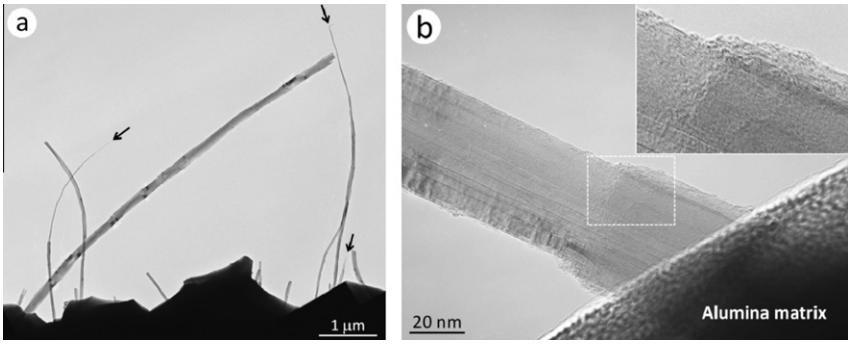

Fig. 3 – TEM images of the fracture surface of the composite acquired (a) low and (b) high magnification images.

failure, and that edges of such outer shells were clearly observed to lie perpendicular to the axis of cylinder, demonstrating the sword-in-sheath failure. Note that MWCNT failure was also observed in fracture surfaces of alumina composites made with arc-discharge-grown and chemical vapor deposition (CVD)-grown MWCNTs prepared under the same processing conditions (Fig. S1 in Supplementary material). The details will be discussed in a separate article. Since no apparent variation in the diameter of the MWCNTs has been observed along the axis in the as-received MWCNTs, these results imply that some MWCNTs underwent failure in the sword-in-sheath manner prior to pullout from the matrix, and no apparent damage appeared to be induced in some of MWCNTs that were not load bearing, as exemplified in Fig. 2b.

The MWCNT failure during crack opening motivated our research of the crack bridging characteristics through the single nanotube pullout tests. We fractured composite specimen by conducting the bending tests, which caused single MWCNT to project from the crack plane. This allows single MWCNT "pickup" with cantilever tip for subsequent tensile loading using the nanomanipulator. As mentioned above, however, the MWCNTs crossing the crack planes were strained during crack opening and possibly underwent failure, as shown in Figs. 2c and d, and 3. Therefore, by observing the fracture surface on the composites, MWCNTs with no apparent damages were selected for the pullout tests.

Results obtained from the pullout experiments revealed that strong load transfer was demonstrated, and no pullout behavior was observed for all 15 MWCNTs tested in this research. Eight of these MWCNTs fractured at the composite surface and the remaining 7 MWCNTs underwent failure in the region between the fixed point on the cantilever and the crack plane, as shown in Fig. 4. Two series of SEM and TEM images for each of two individual MWCNTs, captured before and after their breaking, are shown in Figs. 5 and 6. In the first series (Fig. 5; sample number 14 – see Supplementary Table S1 and Video S1), a MWCNT projecting 5.72 ± 0.01 μm from the fracture surface (Fig. 5a) was "welded" to a cantilever tip by local EBID, and then loaded in increments until failure. The resulting fragment attached on the cantilever tip was at least 10.9 μm long (Fig. 5b), whereas the other fragment remained lodged in a grain boundary of the alumina matrix (Fig. 5c), suggesting that MWCNT underwent failure in a sword-in-sheath manner. TEM images of the broken MWCNT

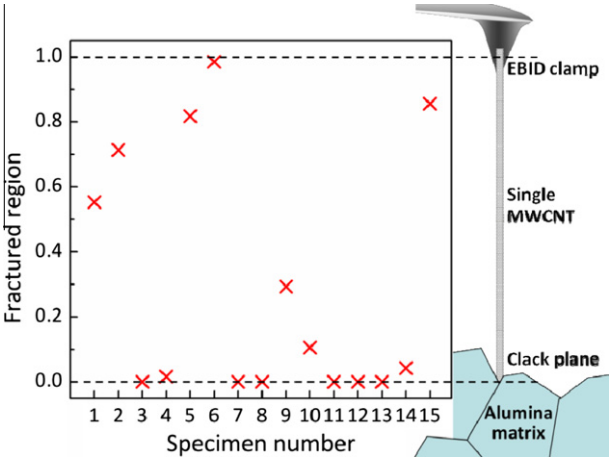

Fig. 4 – Fracture location of single MWCNTs under pullout loading. Of the 15 MWCNTs tested here, 8 MWCNTs fractured on the composite surface (sample numbers: 3, 4, 7, 8, 11–14) and remaining 7 MWCNTs fractured in the middle (sample numbers: 1, 2, 5, 6, 9, 10, and 15).

fragments revealed a variety of structural patterns. They are presented as examples of what happens as a result of loading to break. Images show a change in diameter at location where the MWCNT underwent failure, and that the inner core protruding from the outer shells has a multi-walled closed-end structure, as shown in Fig. 5d and e, respectively. (Given that uniformity of the interwall spacing of 0.34-nm-thick cylinder structure, approximately 11 shells underwent failure.) There results strongly suggest that the MWCNTs broke in the outer shells and the inner core was then completely pulled away, leaving the companion fragment of the outer shells in the matrix.

The sword-in-sheath failure did not always occur. Instead a few MWCNT failed leaving either a very short sword-in-sheath failure or a clean break. As for one example (Fig. 6; sample number 10 – see Supplementary Table S1 and Video S2), a MWCNT projecting 5.34 ± 0.01 μm from the crack plane (Fig. 6a) underwent failure on the composite fracture surface. The resulting fragment attached on the cantilever tip (Fig. 6b) was at least 5.7 μm long, and no fragment was observed at the original position on the crack plane, suggesting that in this case the MWCNT failed by breaking inside the matrix, and did not pull out. Fig. 6c shows the TEM image of the tip of

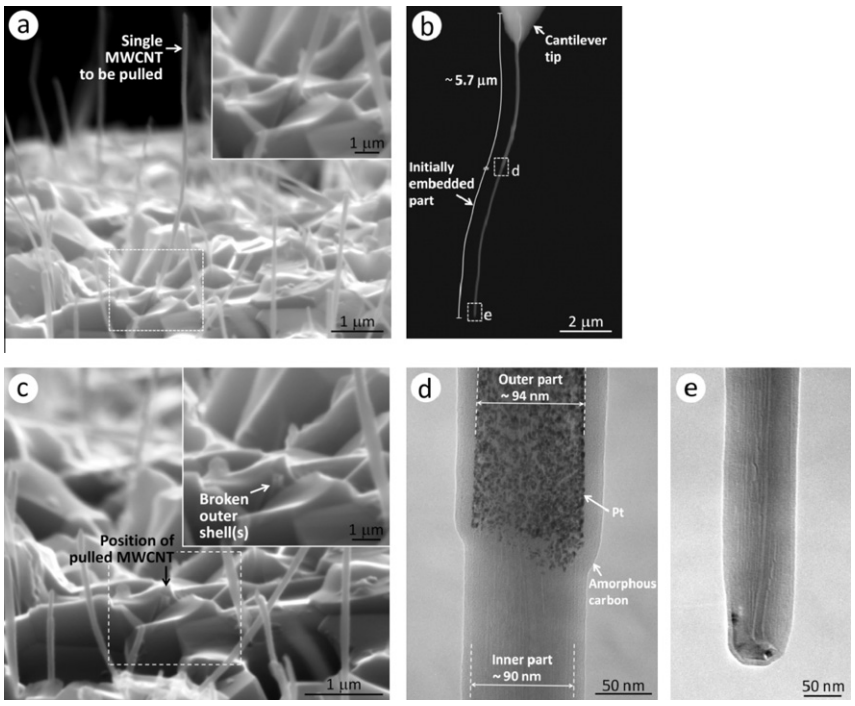

Fig. 5 – SEM images show (a) a free-standing MWCNT having a 5.72 ± 0.01 μm-long on the fracture surface of the composite. (b) After breaking, one fragment of the same MWCNT attached on the cantilever tip had a length ~10.9 μm. (c) The other fragment remained in the matrix. (d,e) TEM images show a change in diameter at location where the MWCNT underwent multi-wall failure, and that it clearly has a multi-walled closed-end structure.

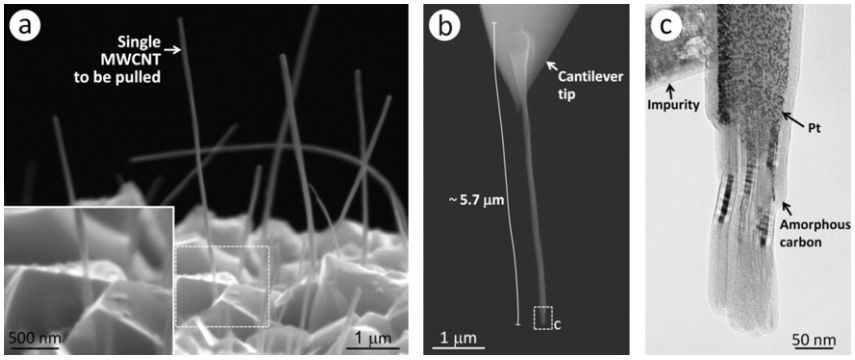

Fig. 6 – In the second series, (a) a tensile-loaded MWCNT with a length of 4.46 ± 0.01 μm fractured on the crack plane. (b) The resulting fragment on the cantilever tip had a length ~5.7 μm. (c) TEM image shows the MWCNT which underwent the very short sword-in-sheath failure or clean break.

the same MWCNT which underwent very short sword-in-sheath failure or clean break during crack opening.

In each case the MWCNTs underwent multi-wall failure bearing load of 19.7 ± 2.1 μN for the sample number 14 and 16.9 ± 2.0 μN for the sample number 10, respectively. The reader is referred to a full list of the MWCNTs tested in the pullout experiments in Table S1 in Supplementary material that shows the geometry, breaking force, fracture strength, and other properties. Considering mean failure force for the 15 samples tested, of 14.4 μN, it reveals a increase in the sustainable load by factors of 19.5 [19], 6.8 [7], and 2.2 [17], compared with mean failure resistance of MWCNTs under tensile loading. The enhancement in the failure load is not clear so far. According to the current TEM observations on MWCNTs protruding from the fracture surface, structural changes and deformations from constant-diameter cylinders (such as occur due to a radial compressive stress of the MWCNT that comes from the difference of coefficients of thermal expansion between MWCNT and ceramics matrix) were frequently observed (see Fig. S2 in Supplementary material) and were not present in the as-received MWCNTs. As per Yu et al. [19] and Peng et al. [7], the outer most shell of MWCNTs was evidently carrying the load under tensile loading and an inner core was not load bearing. Thus, multi-wall failure of MWCNTs observed in this research suggests that some enhancement of load transfer to inner shells may be

facilitated in particular locations through above mentioned structural irregularities.

Next, we schematically describe possible processes and mechanics, explaining the MWCNT failure during crack opening (Fig. 7). As for one example, considering the sample number 14 (Fig. 5), the initial state of the MWCNT in an ideal case is a completely impregnated and isolated embedded in the matrix (Fig. 7a). Tensile stresses parallel to the axis of MWCNT length lead to matrix crack formation. Subsequently, interfacial debonding between two phases may occur (Fig. 7b), perhaps over a limited distance (but this is unlikely to make a major contribution to the fracture energy). Since there is variability in MWCNT strength in the debonded region on either side of the crack plane, and it is possible for the MWCNT to break at a certain position, when the stress in the MWCNT reaches a critical value. As displacement increases, the MWCNTs, rather than pulling out from the alumina matrix, undergo failure in the outer shells and the inner core is pulled away, leaving the fragments of the outer shells in the matrix (Fig. 7c and d).

The reinforcement–matrix interface is usually characterized by the critical shear stress needed to debond the interface and the subsequent shear resistance for a relative sliding of the reinforcement and matrix. When the maximum shear stress reaches the interface shear strength τ_b, the debonding at the reinforcement–matrix interface occurs, and then the reinforcement is pulled out. The corresponding critical pulling force is

$$F^{\tau}_{max} = \tau_b \cdot \pi D L_{emb}, \quad (1)$$

where D is the diameter of the reinforcement, and L_{emb} is the embedded length in the matrix. On the other hand, reinforcement failure occurs when the maximum axial nominal stress reaches reinforcement strength σ_f, and the corresponding critical breaking force is

$$F^{\sigma}_{max} = \sigma_f A_f, \quad (2)$$

where A_f is the effective cross-sectional area of the reinforcement. When F^{σ}_{max} is larger than F^{τ}_{max}, all reinforcements are debonded at the interfaces and are pulled out without reinforcement failure, i.e., weak interface results in interfacial debonding and reinforcement pullout, whereas a strong interface leads to reinforcement failure. There is some work on direct observations to measure the force required to separate a single MWCNT from polymer matrix composites, however, to our best knowledge no work has been carried out on the measurement of the interfacial shear strength in ceramic composites. Recent investigations conducted by Li and co-workers [25] used molecular dynamics (MD) method to estimate the τ_b between MWCNT and ceramics, in which the estimated τ_b has been reported to be in the range of 1–40 MPa. Considering the sample number 14 (that are applicable to estimate the L_{emb} from the acquired TEM image, as shown in Fig. 5d), the force needed to pull the MWCNT out from the matrix is calculated to be 31 μN, assuming the following values: τ_b = 20 MPa, D = 94 nm, L_{emb} = 5.2 μm. In contrast, the measured F^{σ}_{max} of the same MWCNT was 19.7 ± 2.1 μN. This implies that MWCNTs failure prior to pull-out from the matrix seems to naturally occur. Furthermore, some enhancement in the critical pulling force such as due to the radial compressive stress applied to the MWCNT [26] and the formation of interfacial phase between reinforcement/matrix [27] is expected, i.e., the force required to separate a MWCNT from the matrix is anticipated to be much higher than the above. These results raise a question: if no MWCNT failure took place in this composite, how toughness enhancement could be achieved? The R-curve – i.e., crack growth resistance as a function of crack size – is theoretically given in terms of the material parameters, such as reinforcement volume fraction, reinforcement strength, interfacial shear strength, and Young's modulus of reinforcement and matrix, etc. The critical value of apparent stress intensity factor $(K^a_I)_c$ for a straight-through crack in a semi-infinite body is derived in terms of the bridging stresses on the premise that the bridging length is much smaller than the whole crack length [28], as follow;

$$(K^a_I)_c = K^0_{Ic} + \sqrt{\frac{2}{\pi}} \int_0^{\Delta a} \frac{\sigma_b(x)}{\sqrt{x}} dx, \quad (3)$$

where K^0_{Ic} is the critical stress intensity factor of the matrix (=4.37 MPa $m^{1/2}$), Δa is the crack extension length, and $\sigma_b(x)$ is the homogenized traction on the crack surface as a

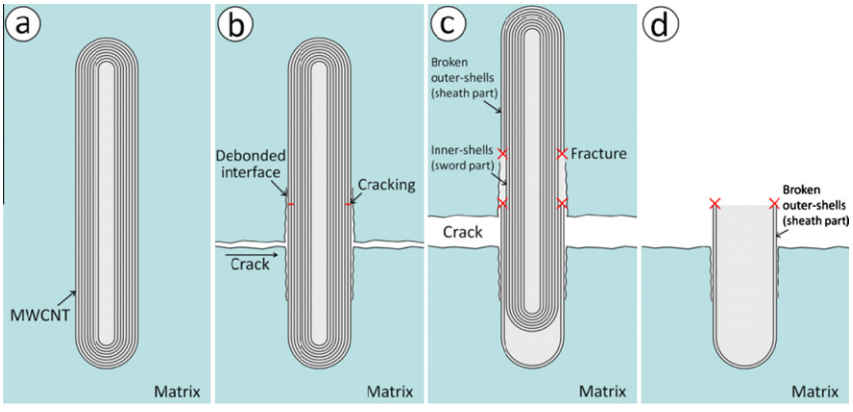

Fig. 7 – Schematic description of possible fracture mechanisms of the MWCNT (sample number 14). (a) Initial state of a MWCNT. (b) Tensile stresses lead to matrix crack and partial debonding formation. (c,d) As displacement increases, the MWCNTs, rather than pulling out from the alumina matrix, undergo failure in the outer shells and the inner core is pulled away, leaving the fragment of the outer shells in the matrix.

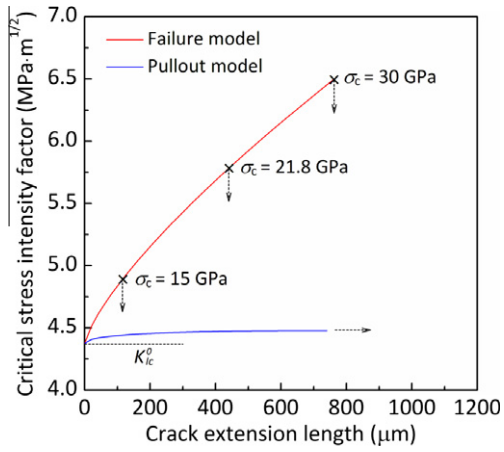

Fig. 8 – Theoretically-calculated crack growth resistance as a function of crack length for the MWCNT/alumina composite.

function of crack opening displacement x [28]. Corresponding to these two failure modes, i.e., toughness enhancement can be earned just by MWCNT failure or MWCNT pullout, there are two types of R-curves as shown in Fig. 8. For MWCNT failure case (similar to failure mode observed in our composite), the $(K_I^a)_c$ estimated with the actual material parameters and the interfacial shear stress of 20 MPa increased up to about 5.8 MPa m$^{1/2}$ until the $\sigma_b(x)$ reached critical MWCNT strength σ_c (=21.8 GPa). As can be seen from examples of Fig. 8, it seems that the use of MWCNT having much higher load carrying capacity is one possible route of achieving tougher MWCNT/ceramic composites. For the MWCNT pullout case, however, the potential for contribution to the fracture toughness enhancement is small. The $(K_I^a)_c$ was increased slightly with an increase in crack length Δa, and then finally going asymptotically to about 4.5 MPa m$^{1/2}$. In this theoretical consideration, MWCNT pullout mode is just the case that if only interface shear strength of 20 MPa is present at the interface of the MWCNTs and the matrix, the fracture toughening effect is very small and could not be improved effectively simply by increasing the MWCNT length, or Young's modulus of MWCNT and matrix. Failure analyses suggest that the direct measurement of the force required to separate a single MWCNT from polycrystalline ceramics will be a fascinating area for further study for fundamental material design of MWCNT/ceramic composites, leading to improved fracture toughness.

Recently Estili et al. have proposed a possible approach for toughening MWCNT/alumina composites, and attempted to engineer strong inter-wall shear resistance in the entire MWCNT structure by embedding MWCNTs in a compressive-stress ceramic environment [29]. They reported that acid-treated MWCNTs with nano-scale defects on their surface underwent multi-wall failure during crack opening in the composite, and claimed that the breaking force of MWCNTs increased dramatically in the compressive-stress ceramic environment. Although the MWCNTs used as the starting materials in their research are the same CNTs as those tested in the present study, their finding of multi-wall failure is based on the use of acid-treated MWCNTs. It has been shown that defects associated with the acid etching can cause stress concentrations and then decrease the strength of the MWCNT [17]. In contrast, our study which used pristine MWCNTs with no acid-etched defects, indicates that multi-wall failure is an intrinsic and inherent characteristic of the MWCNT/alumina composites. As described earlier, multi-wall failure has been confirmed in our recent study for arc-discharge-grown MWCNTs, as well as CVD-grown MWCNTs. Based on this result, we claim that the multi-wall failure is the major cause for the modest enhancement in the fracture properties of MWCNT-based ceramic composites. In addition, no fracture properties have been measured for the acid-treated MWCNTs and the prepared MWCNT/alumina composites prepared in Estili et al. [29]. They conducted only pullout tests on the fracture surface of the composite. Thus, their proposal that residual compressive stress in the alumina matrix is effective in increasing the inter-wall shear resistance and improving the mechanical properties of the composite is based on a qualitative comparison with literature data and may need to be substantiated through direct measurements of the fracture properties (Supporting information can be found in the Supplementary material).

Creating tough, fracture-resistant ceramics has been a central focus of MWCNT/ceramic composites research. Although there are a few papers that report significant improvement in the fracture toughness [30], the improvements by addition of MWCNTs reported in other studies has been limited [31]. The results reported here suggest that modest improvements in toughness reported previously may be due to the way MWCNT's fail during crack opening in the MWCNT/ceramic composites. The design of tougher composites with MWCNTs as a filler will need to account, or in some way circumvent, the sword-in-sheath failure reported here.

4. Conclusions

It has been demonstrated from TEM observations, and single nanotube pullout experiments on the MWCNT/alumina composite having fracture toughness 4.74 ± 0.12 MPa m$^{1/2}$ that strong load transfer was revealed, and no MWCNT pullout behavior was observed. The MWCNTs, rather than pulling out from the alumina matrix, broke in the sword-in-sheath fracture mode, and some MWCNTs failed leaving either the very short sword-in-sheath failure or clean break. We have then also shown that the MWCNTs embedded in the alumina matrix may withstand a much larger tensile load by an inner-walls load-distribution through the structural changes and deformations from constant-diameter cylinders. It was shown from a theoretical analysis assuming the interfacial shear strength of 20 MPa that an important factor affecting the toughness enhancement in our composite was MWCNT strength, and contribution from MWCNT pullout was limited for reinforcement. In totality, our finding suggests important implications for the design of tougher ceramic composites with MWCNTs. The important factor for such tougher ceramic composites will thus be the use of MWCNT having a much higher load carrying capacity (as well as a good dispersion in the matrix).

Acknowledgments

The authors thank Mr. T. Miyazaki of Technical Division, School of Engineering, Tohoku University, for technical assistance in the TEM analysis. This research was partially supported by the Japan Society for the Promotion of Science (JSPS) 08J09683 and by the Grant-in-Aid for Scientific Research (S) 21226004. This work was performed under the inter-university cooperative research program of the Advanced Research Center of Metallic Glasses, Institute for materials Research, Tohoku University. Ruoff group members (J.W.S., J.H.A., R.D.P., R.S.R.) were supported by the NSF #0802247, Fracture Mechanics of Nanowires and Nanostructures, D. Kouris program manager, and the DARPAN/MEMS S&T Fundamentals Program, D. Polla program manager.

Appendix A. Supplementary data

Supplementary data associated with this article can be found, in the online version, at doi:10.1016/j.carbon.2011.04.022.

REFERENCES

[1] Mukerji J. Ceramic matrix composites. Defence Sci J 1993;43(4):385–95.
[2] Evans AG. Perspective on the development of high-toughness ceramics. J Am Ceram Soc 1990;73(2):187–206.
[3] Dai HJ, Wong EW, Lieber CM. Probing electrical transport in nanomaterials: conductivity of individual carbon nanotubes. Science 1996;272(5261):523–6.
[4] Ebbesen TW, Lezec HJ, Hiura H, Bennett JW, Ghaemi HF, Thio T. Electrical conductivity of individual carbon nanotubes. Nature 1996;382(6586):54–6.
[5] Treacy MMJ, Ebbesen TW, Gibson JM. Exceptionally high Young's modulus observed for individual carbon nanotubes. Nature 1996;381(6584):678–80.
[6] Huang JY, Chen S, Wang ZQ, Kempa K, Wang YM, Jo SH, et al. Superplastic carbon nanotubes – conditions have been discovered that allow extensive deformation of rigid single-walled nanotubes. Nature 2006;439(7074):281.
[7] Peng B, Locascio M, Zapol P, Li SY, Mielke SL, Schatz GC, et al. Measurements of near-ultimate strength for multiwalled carbon nanotubes and irradiation-induced crosslinking improvements. Nat Nanotechnol 2008;3(10):626–31.
[8] Peigney A. Composite materials: tougher ceramics with nanotubes. Nat Mater 2003;2(1):15–6.
[9] Sheldon BW, Curtin WA. Nanoceramic composites: tough to test. Nat Mater 2004;3(8):505–6.
[10] Xia Z, Riester L, Curtin WA, Li H, Sheldon BW, Liang J, et al. Direct observation of toughening mechanisms in carbon nanotube ceramic matrix composites. Acta Mater 2004;52(4):931–44.
[11] Schadler LS, Giannaris SC, Ajayan PM. Load transfer in carbon nanotube epoxy composites. Appl Phys Lett 1998;73(26):3842–4.
[12] Qian D, Dickey EC, Andrews R, Rantell T. Load transfer and deformation mechanisms in carbon nanotube–polystyrene composites. Appl Phys Lett 2000;76(20):2868–70.
[13] Barber AH, Cohen SR, Wagner HD. Measurement of carbon nanotube–polymer interfacial strength. Appl Phys Lett 2003;82(23):4140–2.
[14] Flahaut E, Peigney A, Laurent C, Marliere C, Chastel F, Rousset A. Carbon nanotube–metal-oxide nanocomposites: microstructure, electrical conductivity and mechanical properties. Acta Mater 2000;48(14):3803–12.
[15] Yamamoto G, Omori M, Yokomizo K, Hashida T, Adachi K. Structural characterization and frictional properties of carbon nanotube/alumina composites prepared by precursor method. Mater Sci Eng B-Adv 2008;148(1–3):265–9.
[16] Yamamoto G, Omori M, Hashida T, Kimura H. A novel structure for carbon nanotube reinforced alumina composites with improved mechanical properties. Nanotechnology 2008;19(31) [article number: 315708].
[17] Yamamoto G, Suk JW, An JH, Piner RD, Hashida T, Takagi T, et al. The influence of nanoscale defects on the fracture of multi-walled carbon nanotubes under tensile loading. Diam Relat Mater 2010;19(7–9):748–51.
[18] Kim YA, Hayashi T, Endo M, Kaburagi Y, Tsukada T, Shan J, et al. Synthesis and structural characterization of thin multi-walled carbon nanotubes with a partially facetted cross section by a floating reactant method. Carbon 2005;43:2243–50.
[19] Yu MF, Lourie O, Dyer MJ, Moloni K, Kelly TF, Ruoff RS. Strength and breaking mechanism of multiwalled carbon nanotubes under tensile load. Science 2000;287(5453):637–40.
[20] Ding W, Dikin DA, Chen X, Piner RD, Ruoff RS, Zussman E, et al. Mechanics of hydrogenated amorphous carbon deposits from electron-beam-induced deposition of a paraffin precursor. J Appl Phys 2005;98(1) [article number: 014905].
[21] Sader JE, Chon JWM, Mulvaney P. Calibration of rectangular atomic force microscope cantilevers. Rev Sci Instrum 1999;70(10):3967–9.
[22] Ding WQ, Calabri L, Chen XQ, Kohhaas KM, Ruoff RS. Mechanics of crystalline boron nanowires. Compos Sci Technol 2006;66(9):1112–24.
[23] Ding WQ, Guo ZY, Ruoff RS. Effect of cantilever nonlinearity in nanoscale tensile testing. J Appl Phys 2007;101(3):203106.
[24] Barber AH, Andrews R, Schadler LS, Wagner HD. On the tensile strength distribution of multiwalled carbon nanotubes. Appl Phys Lett 2005;87(20) [article number: 203106].
[25] Li LL, Xia ZHH, Curtin WA, Yang YQQ. Molecular dynamics simulations of interfacial sliding in carbon-nanotube/diamond nanocomposites. J Am Ceram Soc 2009;92(10):2331–6.
[26] Jiang DT, Thomson K, Kuntz JD, Ager JW, Mukherjee AK. Effect of sintering temperature on a single-wall carbon nanotube–toughened alumina-based nanocomposite. Scripta Mater 2007;56(11):959–62.
[27] Ahmad I, Unwin M, Cao H, Chen H, Zhao H, Kennedy A, et al. Multi-walled carbon nanotubes reinforced Al_2O_3 nanocomposites: mechanical properties and interfacial investigations. Compos Sci Technol 2010;70(8):1199–206.
[28] Marshall DB, Cox BN, Evans AG. The Mechanics of matrix cracking in brittle-matrix fiber composites. Acta Metallurgica 1985;33(11):2013–21.
[29] Estilli M, Kawasaki A. Engineering strong intergraphene shear resistance in multi-walled carbon nanotubes and dramatic tensile improvements. Adv Mater 2010;22(5):607–10.
[30] Zhan GD, Kuntz JD, Wan J, Mukherjee AK. Single-wall carbon nanotubes as attractive toughening agents in alumina-based nanocomposites. Nat Mater 2002;2:38–42.
[31] Cho J, Boccaccini AR, Shaffer MSP. Ceramic matrix composites containing carbon nanotubes. J Mater Sci 2009;44:1934–51.